follow due to the overlapping nature of the azopyridine and bipyridine absorptions. The band assigned to the azo group shows a reduction in intensity relative to those at 1400 cm^{-1} and is shifted by 20 cm^{-1} to lower energy, consistent with the addition of an electron to the N=N bond (*20, 25*). When the second reduction product is formed, the azo peak at 1304 cm^{-1} disappears and a single relatively more intense band appears to lower energy, at 1295 cm^{-1}. Several changes also occur in the region of 1400–1600 cm^{-1} as shown in Figure 5b, notably a merging of the bands near 1600 cm^{-1} into one broad multiple band at 1602 cm^{-1}. These spectroscopic changes are reversible upon reoxidation to the initial species.

The results reported here have been obtained by use of a gold minigrid working electrode. However, an attractive feature of the cell is that many other electrode materials can be easily incorporated. We have obtained satisfactory spectroelectrochemical performance by using windows coated with a conducting layer of tin oxide or thin carbon film as the working electrode. Similarly, the cell may readily be used with semitransparent metal film electrodes, or other electrode materials, such as platinum gauze.

In summary, the thin-layer cell described here has several advantages over many previous cell designs. These include versatility of the spectroscopic range and electrode material, good electrochemical behavior, ease of cleaning and assembly, and suitability for use with aqueous or organic solutions. In particular, the cell allows the convenient and rapid acquisition of infrared data on redox species, an area which has been neglected in the past, but which can provide important information concerning the nature of the redox species and the electrochemical processes taking place.

No problems were experienced in recording the spectra of air-sensitive materials even though there is evidence that Teflon is somewhat permeable to oxygen. Where extrene air sensitivity is a problem, Kel-F might be used for the spacer material.

ACKNOWLEDGMENT

We are grateful to Shafi Greenberg and Wei Liu for help with the synthesis of complexes.

LITERATURE CITED

(1) Kuwana, T.; Winograd, N. In *Electroanalytical Chemistry*; Bard, A. J., Ed.; Marcel Dekker: New York, 1974; Vol. 7, p 1.
(2) Heineman, W. R.; Hawkridge, F. M.; Blount, H. N. In *Electroanalytical Chemistry*; Bard, A. J., Ed.; Marcel Dekker: New York, 1984; Vol. 13, p 1.
(3) Robinson, J. In *Electrochemistry—Specialist Periodical Reports*; Pletcher, D., Ed.; The Royal Society of Chemistry, Burlington House: London, 1984; Vol. 9, p 101.
(4) Enger, S. K.; Weaver, M. J.; Walton, R. A. *Inorg. Chim. Acta* **1987**, *129*, L1.
(5) Bullock, J. P.; Boyd, D. C.; Mann, K. R. *Inorg. Chem.* **1987**, *26*, 3084.
(6) Finklea, H. O.; Boggess, R. K.; Trogdon, J. W.; Schultz, F. A. *Anal. Chem.* **1983**, *55*, 1177.
(7) Lin, X. Q.; Kadish, K. M. *Anal. Chem.* **1985**, *57*, 1498; **1986**, *58*, 1493.
(8) Scherson, D. A.; Sarangapani, S.; Urbach, F. L. *Anal. Chem.* **1985**, *57*, 1501.
(9) Hobart, D. E.; Norvell, V. E.; Varlashkin, P. G.; Hellwege, H. E.; Peterson, J. R. *Anal. Chem.* **1983**, *55*, 1634.
(10) Zak, J.; Porter, M. D.; Kuwana, T. *Anal. Chem.* **1983**, *55*, 2219.
(11) Condit, D. A.; Herrera, M. E.; Stankovich, M. T.; Curran, D. J. *Anal. Chem.* **1984**, *56*, 2909.
(12) Kobayashi, N.; Nishiyama, Y. *J. Phys. Chem.* **1985**, *89*, 1167.
(13) Smith, D. A.; Elder, R. C.; Heineman, W. R. *Anal. Chem.* **1985**, *57*, 2361.
(14) Gui, Y.-P.; Kuwana, T. *Langmuir* **1986**, *2*, 471.
(15) Sanderson, D. G.; Anderson, L. B. *Anal. Chem.* **1986**, *57*, 2388.
(16) Heineman, W. R.; Burnett, J. N.; Murray, R. W. *Anal. Chem.* **1968**, *40*, 1974.
(17) Shoemaker, D. P.; Garland, C. W.; Steinfeld, J. I. *Experiments in Physical Chemistry*, 3rd ed.; McGraw-Hill: New York, 1974; p 677.
(18) Bailey, P. L. *Analysis with Ion-Selective Electrodes*; Heyden: London, 1976; p 20.
(19) Leznoff, C. C.; Marcuccio, S. M.; Greenberg, S.; Lever, A. B. P.; Tomer, K. B. *Can. J. Chem.* **1985**, *63*, 623.
(20) Nevin, W. A.; Liu, W.; Haga, M.; Lever, A. B. P., to be submitted for publication.
(21) Hubbard, A. T.; Anson, F. C. In *Electroanalytical Chemistry*; Bard, A. J., Ed.; Marcel Dekker: New York, 1970; Vol. 4, p 129.
(22) Bard, A. J.; Faulkner, L. R. *Electrochemical Methods: Fundamentals and Applications*; Wiley: New York, 1980.
(23) Nyokong, T.; Gasyna, Z.; Stillman, M. J. *Inorg. Chem.* **1987**, *26*, 548.
(24) Wolfgang, S.; Strekas, T. C.; Gafney, H. D.; Krausz, K. *Inorg. Chem.* **1984**, *23*, 2650.
(25) Goswami, S.; Chakraverty, A. R.; Chakravorty, A. *Inorg. Chem.* **1983**, *22*, 602.

RECEIVED for review June 8, 1987. Accepted November 8, 1987. We thank the Natural Sciences and Engineering Research Council (Ottawa, Canada) and the Office of Naval Research (Washington, DC) for financial support.

High-Sensitivity Absorbance Determination by Laser-Induced Thermal Modulation of Electrical Conductivity

Robert McLaren and Norman J. Dovichi*

Department of Chemistry, University of Alberta, Edmonton, Alberta, Canada T6G 2G2

The determination of absorbance has remained a very powerful and important technique in qualitative and quantitative analysis. Spectral variations in absorbance are used to infer the structure of the analyte and Beer's law is used to relate absorbance with analyte concentration. Conventionally, absorbance, A, is determined from the transmission, T, of a sample

$$A = \epsilon bC = -\log T = \log (P_0/P) \quad (1)$$

where ϵ is the molar absorptivity of the sample, b is path length, C is analyte concentration in moles per liter, P_0 is the incident light power, and P is the transmitted light power. For very weakly absorbing analyte, Beer's law may be approximated with a power series expansion

$$A = \frac{P_0/P - 1}{2.303} = \frac{\Delta P}{2.303} \quad (2)$$

where $\Delta P = (P_0 - P)/P$ is the relative change in light power upon transmission through the sample. The absorbance detection limit is proportional to the relative precision with which the light power may be determined. By use of conventional instrumentation, the light power may be determined with a relative precision of ca. 1 part per thousand. With care, the light power may be determined to 1 part in ten thousand, and with extreme care, light power may be determined to 1 part in one hundred thousand (*1, 2*). Absorbance detection limits less than 10^{-5} appear beyond the state-of-the-art using transmission measurements.

To improve absorbance detection limits, it is advantageous to detect signals associated with photophysical processes which occur after absorbance. For example, excellent detection limits may be obtained by means of laser-induced fluorescence. The state-of-the-art detection limit for fluorescence, 8.9×10^{-14} M rhodamine 6G in a 30-μm diameter sample stream (*3*), corresponds to an absorbance detection limit of 1.7×10^{-11} across the stream diameter. Clearly, fluorescence measure-

0003-2700/88/0360-0730$01.50/0

ments provide a significant improvement in absorbance detection limit compared with transmission measurements. Of course, this improvement arises because the fluorescence signal is detected on a weak Raman background so that high power excitation may be employed. On the other hand, an increase in light power produces no change in the sensitivity of a transmission measurement. Unfortunately, fluorescence is of limited utility since relatively few molecules possess significant quantum yield of fluorescence (*4*).

To improve absorbance detection limits for molecules with insignificant fluorescence quantum yield, it is possible to detect a temperature rise associated with nonradiative relaxation of excited states. A class of high-sensitivity absorbance techniques have been developed based upon measurement of this temperature rise. These thermal absorbance techniques offer an important property: an arbitrarily transparent material will give rise to a measurable temperature rise simply by utilization of an arbitrarily powerful light source (if you push hard enough, it will fall over). The most simple thermal absorbance determination relies upon a direct measurement of the temperature rise with a thermocouple (*5*). Other thermal absorbance techniques utilize indirect measurement of the temperature rise within the sample wherein some property of the sample which undergoes a change with temperature is monitored. The two most common thermal absorbance techniques are photoacoustic spectroscopy, which utilizes a measurement of the change in density produced by the rise in sample temperature, and thermooptical methods, which detect a change in the refractive index of the solvent produced by the temperature rise associated with absorbance (*6–11*). Another thermal absorbance technique relies upon variatons in electron capture cross-section with temperature for gas-phase analysis (*12*).

In thermooptical measurements, the signal is proportional to the product of the temperature rise and the change in refractive index with temperature for the solvent. The best liquid phase thermooptical absorbance detection limits are on the order of 10^{-7} for a 1-cm path length using a single beam thermal lens instrument and 3×10^{-9} for a 2-μm path length using a crossed-beam thermal lens instrument (*13,14*). However, these detection limits were obtained for nonpolar organic solvents or mixed water–alcohol solvents and with a 100-mW laser. The change in refractive index with temperature for water is 1 to 2 orders of magnitude smaller than that of organic liquids; relatively poor detection limits are produced for aqueous samples by thermooptical measurements.

Inspection of a table of physical properties of solvents and solutes reveals many properties which change with temperature. For example, surface tension and sound velocity both undergo a relative change of a part per thousand per degree temperature rise for many solvents (*15*). An example of a physical property for most solvents with a rather large temperature dependence is viscosity, which undergoes a relative change of a few percent per degree temperature change. This sensitivity is at least an order of magnitude higher than that observed in thermal lens or photoacoustic measurements. For water, the relative temperature dependence of viscosity is nearly 3 orders of magnitude higher than that of refractive index!

At first glance, thermal measurements of viscosity would appear to be a formidable challenge. After all, viscosity is conventionally measured by flow rate through a calibrated capillary tube, or by a concentric tube viscometer, or by the velocity of a sphere falling through the liquid. However, viscosity is also related to a number of important physical properties of solutions. In particular, the electrical conductivity of a solution is proportional to the velocity at which ions migrate under the influence of an electric field, which, in turn, is inversely proportional to the viscosity of the solution. Therefore, the change in electrical conductivity induced by the temperature rise following absorbance of light may be used as a sensitive measurement of absorbance. This technique offers sufficiently high sensitivity so that low power and inexpensive lasers may be employed as light sources. We anticipate that the very high sensitivity produced by thermal modulation of electrical conductivity (TMEC) will prove to be a particularly powerful and useful technique for determination of minute absorbance within aqueous samples. Furthermore, TMEC foreshadows a larger class of absorbance determinations based upon thermal modulation of other electrochemical processes.

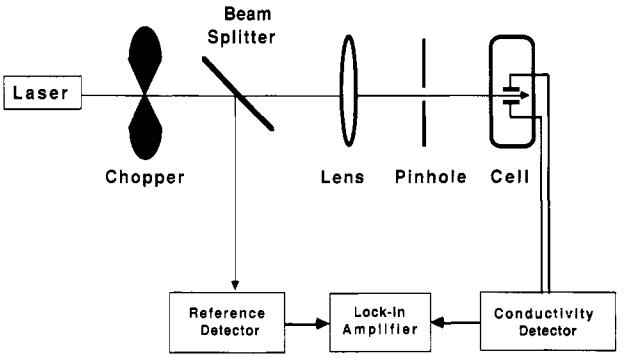

Figure 1. Experimental diagram: laser is a 4-mW helium–neon laser and the lens is an 18× microscope objective.

EXPERIMENTAL SECTION

Apparatus. A block diagram of the preliminary instrument for TMEC is presented in Figure 1. The apparatus was constructed on a 3 ft by 4 ft optical breadboard, Melles Griot model 07 OBB 012. A helium–neon laser, Melles Griot, delivered to the sample a 4-mW beam at 632.8 nm wavelength. The intensity of this beam was modulated in a square wave with a variable-frequency mechanical chopper. A small portion, ca. 5%, of the beam intensity was directed with a microscope slide beam splitter to a reference photodiode, described below. The major portion of the beam was focused into the detector cell with an 18×, 10-mm focal length microscope objective. A mask, consisting of a 1-mm aperture, was placed in the beam path to reduce the amount of scattered laser light illuminating the electrodes.

The detector cell was primarily designed for ease of construction. The electrodes were made from insulated 32-gauge wire, 0.20-mm diameter. A ca. 20-cm length of wire was formed into a loop, with the ends twisted together. A glass capillary tube was forced over the twisted ends of the wire and positioned near the loop. After the wire was epoxied in the capillary, the loop of wire was slit with a razor blade, producing a 0.24-mm gap between the ends of the wire. The wire electrode was then epoxied to the inside wall of a Pasture pipet, Chase Instruments, Inc. The bottom of the pipet was connected to a drain tube for ease of sample introduction and replacement. The pipet was mounted on a three-axes translation stage system to allow convenient positioning with respect to the laser beam waist.

The electronics associated with the conductivity detector are shown in Figure 2. A function generator, Hewlett-Packard Model 3311A, was used to generate a variable-frequency, variable-voltage sine wave for presentation to the electrodes. The ac voltage amplitude produced by the function generator was monitored with a digital multimeter, Simpson Model 461. The signal from the function generator was passed through a 0.47-μF capacitor to remove any direct current offset. Coaxial cable was used to connect the electrodes to the remainder of the electronic circuit. The current passing through the cell was conditioned with a current-to-voltage converter constructed from a LF351 JFET operational amplifier with a 270-kΩ feedback resistor in parallel with a 5-pF capacitor.

The ac voltage at point A in the circuit is proportional to the conductivity of the solution. The remaining portion of the circuit acts as a half-wave rectifier plus a low-pass filter to both demodulate and smooth the conductivity signal for presentation to

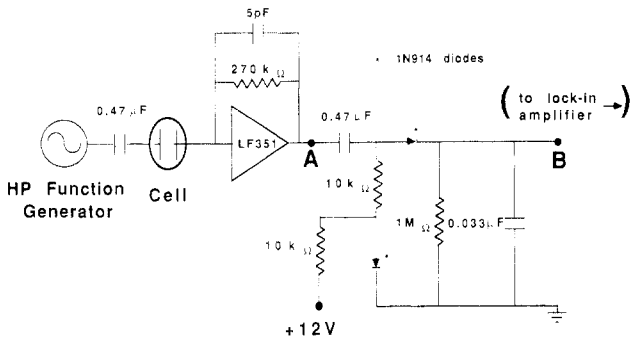

Figure 2. Electronic diagram. Asterisks indicate 1N914 diodes.

the lock-in amplifier at point B. In essence, a low-frequency modulation due to laser-induced heating of the sample and a concomitant change in electrical conductivity is induced upon the high-frequency carrier wave of the ac voltage. Other approaches to signal demodulation may be envisioned for future work.

The signal from the conductivity detector was sent to a two-phase lock-in amplifier, Ithico Model 3961, operating in the amplitude mode with a 3-s time constant. The reference signal was generated by the reference photodiode, whose output was conditioned with a current-to-voltage converter constructed with a LF 351 JFET operational amplifier with a 15-kΩ feedback resistor in parallel with a 100-pF capacitor.

Alignment. To minimize the background signal associated with stray light striking the electrodes, the beam waist was located in the gap between the electrodes. To achieve this alignment, the sample cuvette was mounted on a three-axis translation stage. Inspection of the beam profile on a piece of paper placed about a meter past the cuvette revealed a diffraction pattern associated with the interaction of the beam and the electrodes. To align the system, the electrodes were centered about the beam axis some distance past the beam waist. This step ensured that the electrodes were centered vertically with respect to the beam axis. Next, the electrode was translated toward the lens until the beam profile revealed no interaction between the beam and the electrodes.

Chemicals. The conductivity detector was first characterized by calibration against an aqueous sodium chloride solution. In the thermal modulation experiments, methylene blue was utilized as the absorbing species. Mixed 90/10 water/methanol (v/v) solvent was employed for the absorbance detector. A small amount of methanol was used in the solvent to minimize adsorption of the dye upon the cuvette walls. Typically, the solutions were made a constant 0.05 M NaCl to act as an electrolyte. The solutions were passed through a 0.22-μm filter before use.

RESULTS AND DISCUSSION

The instrument was first characterized with respect to conventional conductivity measurements. The conductivity of a series of aqueous sodium chloride solutions was measured, using a 20-kHz carrier frequency. The conductivity of the solution was linearly related to salt concentration, $r > 0.9999$, up to a salt concentration of 0.05 M. Loading of the voltage source occurred at higher salt concentration, leading to negative deviations from linearity. The signal was also investigated as a function of carrier wave voltage for a 0.05 M aqueous sodium chloride solution and a 0.05 M sodium chloride/10^{-5} M methylene blue solution. The signal was linearly related to carrier wave voltage up to about 3 V (root mean square). A slight positive curvature was noted at higher voltages, presumably related to electrochemistry occurring at the electrodes. A carrier wave voltage of 2.0 V was employed for all other experiments. Last, the variation in signal with carrier wave frequency was investigated. Typically, a carrier frequency on the order of 20 kHz was employed from the function generator. Lower frequencies produced poorer signal-to-noise ratio, presumably due to $1/f$ noise, whereas stray capacitance and inductance associated with the circuit become significant at higher frequencies.

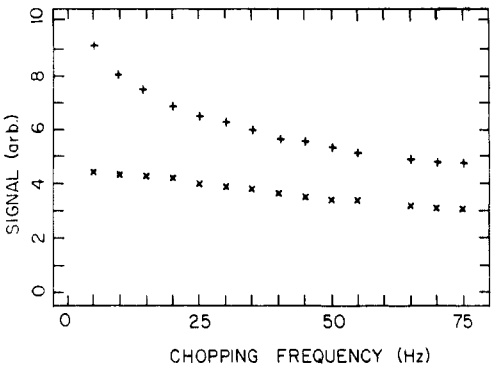

Figure 3. Laser chopping frequency dependence of thermal-modulated electrical conductivity signal. The background signal corresponds to the symbol X and the signal obtained with a 2.5×10^{-5} M dye solution corresponds to the symbol +. No data were obtained at 60 Hz due to interference from line frequency. The uncertainties in the data are smaller than the symbols.

To characterize TMEC, the laser-induced modulation signal was studied as a function of laser chopping frequency, Figure 3. The signal decreases rapidly with an increase in chopping frequency when the cell was filled with a relatively high dye concentration. This role-off signal at higher frequencies is typical of other thermooptical phenomena, particularly thermal lens measurements (*16, 17*). To maximize the TMEC signal, it is necessary to utilize a low chopping frequency. The rate of decrease in signal with modulation frequency is interesting; consideration of the expected laser beam waist spot size, about 5-μm, produced by the 10-mm focal length microscope objective and this laser leads to an expected thermal time constant of about 4 ms. Instead, the rapid decrease in signal with modulation frequency is consistent with a thermal time constant associated with a much larger solvent volume. This modulation frequency data suggest that it is necessary to heat most of the solution between the electrodes in order to obtain a significant TMEC signal.

A significant background signal was obtained with a highly transparent, pure solvent. This signal was several orders of magnitude larger than would be produced by background absorbance by the solvent. Since methylene blue often adsorbs strongly to glass, it is possible that the background signal is associated with solvent contamination. However, inspection of the chopping frequency dependence of the background signal suggests a much larger source of background signal: scattered laser light reaching the electrodes. The slow decrease in background signal with chopping frequency suggests a short time constant, consistent with the high thermal diffusivity of copper which is roughly a factor of 700 larger than that of water. Furthermore, the background signal increased by several orders of magnitude when the electrodes were illuminated directly with the laser beam. In fact, an increase in background signal was observed for unfiltered solutions, presumably due to an increase in scattered light reaching the electrodes. Use of low modulation frequencies maximizes the signal to background ratio.

A calibration curve was constructed for methylene blue in 90/10 water/methanol. The signal is linear from the detection limit, 2σ, of 2×10^{-7} M to at least 10^{-5} M, $R > 0.999$. The deviation from linearity at higher concentrations is associated with several factors, including formation of dimers and trimers of the dye (*18–20*) and a decrease in laser power due to absorbance occurring between the cuvette windows and the electrodes. The latter effect has been observed for thermooptical techniques (*17, 21*).

CONCLUSIONS

TMEC produces absorbance detection limits which are similar to other thermooptical measurements in water. On

the one hand, the sensitivity of the measurement is high because of the large change in electrical conductivity with temperature for aqueous samples. On the other hand, two factors lead to degradation of precision. First, electrical conductivity is not usually measured with high precission. The major difficulty in conductivity measurements, in fact, is temperature sensitivity. Some of the low-frequency temperature drift which plagues electrical conductivity measurements should be attenuated at the low audio frequencies employed in the TMEC measurements. It is expected that higher modulation frequencies, employed with narrower gap electrodes, will greatly improve the precision of the measurement.

A second source of reduced precision in TMEC measurements is a large background signal associated with illumination of the electrodes by stray laser light. This phenomenon is similar to that observed in photoacoustic spectroscopy. As in photoacoustic spectroscopy, minimization of the background signal will result from incremental improvements in the laser beam quality and shielding of scattered laser light. One potential solution is to utilize an electrodeless conductivity detector (*22*).

Applications of the thermally modulated electrical conductivity detector will be found whenever high sensitivity measurements of absorbance must be made, particularly in aqueous samples. One advantage of the technique is the small volume in which the measurement may be performed. The volume between the two electrodes employed in our crude instrument is on the order of 10 nL. At the detection limit, only 2 fmol of analyte is present between the electrodes. Improvements in the electrode configuration should produce detection volumes at least an order of magnitude smaller. Applications of the high sensitivity detector may be envisioned in both capillary liquid chromatography and capillary zone electrophoresis. In particular, the latter technique has been combined with minaturized conductivity detectors (*23*, *24*). It should be possible to introduce a laser beam between the electrodes for simultaneous absorbance and conductivity detection in capillary zone electrophoresis.

Additional sensitivity for the thermally modulated electrical conductivity may be possible by taking advantage of the shift in equilibrium with temperature for weak acids at room temperature. Both carbonic acid (k_1) and boric acid undergo a 2% change in ionization constant per degree (*15*) and the autoprotolysis constant for water undergoes a 6% increase per degree temperature rise at room temperature (*25*). It should be possible to double the sensitivity of the TMEC measurement by utilizing an appropriate buffer, hence combining ionization and conductivity temperature dependence of the solvent system.

TMEC forms the first example of a potentially very large class of absorbance determinations based upon thermal modulation of electrochemical processes. For example, the potential of a half-cell undergoes a relative change with temperature which is inversely proportional to the absolute temperature; at room temperature, the relative change in potential of a cell is about 0.3% per degree, roughly comparable to thermooptical techniques. Either the absorbance associated with colored material in solution or adsorbed directly upon the electrode could give rise to the thermal modulated signal. Application with microelectrodes should result in high-precision, low-volume measurements of both electrochemistry and absorbance.

Thermooptical measurements based upon mirage spectroscopy and the gradient-sensitive technique have been performed at electrodes (*26*, *27*). In these experiments, the electrochemical process perturbs the thermooptical signal. However, in thermal modulation of electrochemical processes, the thermal changes associated with absorbance would be related to a perturbation in the electrochemical measurement. Since only a single light beam is employed in the thermal modulation of electrochemical processes, the technique should demonstrate greater simplicity compared with those thermooptical techniques which utilize two laser beams.

LITERATURE CITED

(1) Pardue, H. L.; Rodriguez, P. A. *Anal. Chem.* **1967**, *39*, 901-903.
(2) Kaye, W. *Anal. Chem.* **1981**, *53*, 369-374.
(3) Dovichi, N. J.; Martin, J. C.; Jett, J. H.; Trkula, M.; Keller, R. A. *Anal. Chem.* **1984**, *56*, 348-354.
(4) Hirschfeld, T. *Appl. Spectrosc.* **1977**, *31*, 238.
(5) Brilmyer, G. H.; Bard, A. J. *Anal. Chem.* **1980**, *52*, 685-691.
(6) Kreuzer, L. B. *Anal. Chem.* **1974**, *46*, 235A-244A.
(7) Rosencwaig, A. *Anal. Chem.* **1975**, *47*, 592A-604A.
(8) Harris, J. M.; Dovichi, N. J. *Anal. Chem.* **1980**, *52*, 695A-706A.
(9) Whinnery, J. R. *Acc. Chem. Res.* **1974**, *7*, 225-231.
(10) Jackson, W. B.; Amer, N. M.; Boccara, A. C.; Fournier, D. *Appl. Opt.* **1981**, *20*, 1333-1344.
(11) Dovichi, N. J. *CRC Crit. Rev. Anal. Chem.* **1987**, *17*, 357-423.
(12) Dovichi, N. J.; Keller, R. A. *Anal. Chem.* **1983**, *55*, 543-549.
(13) Dovichi, N. J.; Harris, J. M. *Anal. Chem.* **1981**, *53*, 106-109.
(14) Nolan, T. G.; Dovichi, N. J. *IEEE Circuits Devices Mag.* **1986**, *2*, 54-56.
(15) *CRC Handbook of Chemistry and Physics*, 51st Ed.; Weast, R. C., Ed.; CRC Press: Boca Raton, FL, 1970; Sections D and F.
(16) Dovichi, N. J.; Harris, J. M. *Proc. SPIE-Int. Soc. Opt. Eng.* **1981**, *288*, 372-375.
(17) Nolan, T. G.; Weimer, W. A.; Dovichi, N. J. *Anal. Chem.* **1984**, *56*, 1704-1707.
(18) Braswell, E. H. *J. Phys. Chem.* **1984**, *88*, 3653-3658.
(19) Rabinowitch, E.; Epstein, L. F. *J. Am. Chem. Soc.* **1941**, *63*, 69-78.
(20) Braswell, E. *J. Phys. Chem.* **1968**, *72*, 2477-2483.
(21) Wetsel, G. C.; Stotts, S. A. *Appl. Phys. Lett.* **1983**, *42*, 931-933.
(22) Shaw, R.; Light, T. S. *ISA Trans.* **1982**, *21*, 63-70.
(23) Huang, X. H.; Pang, T. K. J.; Gordon, M. J.; Zare, R. N. *Anal. Chem.* **1987**, *59*, 2747-2749.
(24) Mikkers, F. E. P.; Everaerts, F. M.; Verheggen, Th. P. E. M. *J. Chromatogr.* **1979**, *169*, 1-10.
(25) Light, T. S.; Licht, S. L. *Anal. Chem.* **1987**, *59*, 2327-2330.
(26) Tamor, M. A.; Hetrick, R. E. *Appl. Phys. Lett.* **1985**, *46*, 460-462.
(27) Pawliszyn, J.; Weber, M. F.; Dignam, M. J.; Mandelis, A.; Venter, R. D.; Park, S. U. *Anal. Chem.* **1986**, *58*, 239-242.

RECEIVED for review August 3, 1987. Accepted November 24, 1987. This work was funded by the National Sciences and Engineering Research Council of Canada.

Determination of Selenium and Tellurium in Copper Standard Reference Materials Using Stable Isotope Dilution Spark Source Mass Spectrometry

E. S. Beary,* P. J. Paulsen, and G. M. Lambert

National Bureau of Standards, Center for Analytical Chemistry, Inorganic Analytical Research Division, Gaithersburg, Maryland 20899

The levels of certain trace elements in high-purity copper, including selenium (Se) and tellurium (Te), are important because even small variations can significantly alter such properties as conductivity and malleability. In the middle 1970s, an isotope dilution spark source mass spectrometric (IDSSMS) procedure was developed for the certification of